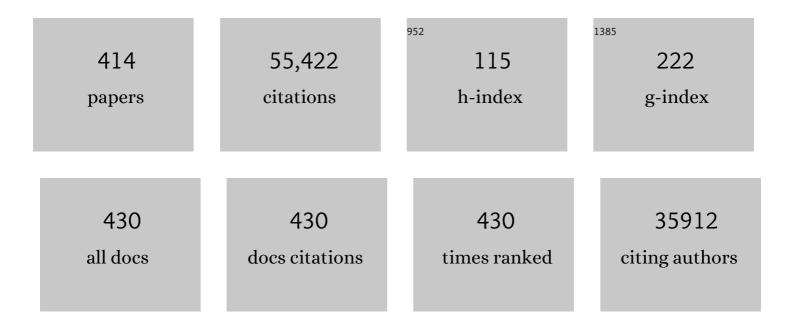
Raymond C Stevens

List of Publications by Year in descending order

Source: https://exaly.com/author-pdf/4560883/publications.pdf Version: 2024-02-01



#	Article	IF	CITATIONS
1	High-Resolution Crystal Structure of an Engineered Human β ₂ -Adrenergic G Protein–Coupled Receptor. Science, 2007, 318, 1258-1265.	12.6	3,112
2	The 2.6 Angstrom Crystal Structure of a Human A _{2A} Adenosine Receptor Bound to an Antagonist. Science, 2008, 322, 1211-1217.	12.6	1,688
3	Structures of the CXCR4 Chemokine GPCR with Small-Molecule and Cyclic Peptide Antagonists. Science, 2010, 330, 1066-1071.	12.6	1,610
4	GPCR Engineering Yields High-Resolution Structural Insights into β ₂ -Adrenergic Receptor Function. Science, 2007, 318, 1266-1273.	12.6	1,324
5	Influenza Neuraminidase Inhibitors Possessing a Novel Hydrophobic Interaction in the Enzyme Active Site:Â Design, Synthesis, and Structural Analysis of Carbocyclic Sialic Acid Analogues with Potent Anti-Influenza Activity. Journal of the American Chemical Society, 1997, 119, 681-690.	13.7	1,061
6	Structure of the Human Dopamine D3 Receptor in Complex with a D2/D3 Selective Antagonist. Science, 2010, 330, 1091-1095.	12.6	1,034
7	Structure-Function of the G Protein–Coupled Receptor Superfamily. Annual Review of Pharmacology and Toxicology, 2013, 53, 531-556.	9.4	907
8	A Specific Cholesterol Binding Site Is Established by the 2.8 à Structure of the Human β2-Adrenergic Receptor. Structure, 2008, 16, 897-905.	3.3	892
9	Structural Basis for Allosteric Regulation of GPCRs by Sodium Ions. Science, 2012, 337, 232-236.	12.6	860
10	Structure of the human \hat{I}^{e} -opioid receptor in complex with JDTic. Nature, 2012, 485, 327-332.	27.8	797
11	Structure of an Agonist-Bound Human A _{2A} Adenosine Receptor. Science, 2011, 332, 322-327.	12.6	783
12	Protein production and purification. Nature Methods, 2008, 5, 135-146.	19.0	763
13	Structure of the human histamine H1 receptor complex with doxepin. Nature, 2011, 475, 65-70.	27.8	727
14	Crystal structure of botulinum neurotoxin type A and implications for toxicity. Nature Structural Biology, 1998, 5, 898-902.	9.7	687
15	Crystal structure of rhodopsin bound to arrestin by femtosecond X-ray laser. Nature, 2015, 523, 561-567.	27.8	683
16	Biased Signaling Pathways in β ₂ -Adrenergic Receptor Characterized by ¹⁹ F-NMR. Science, 2012, 335, 1106-1110.	12.6	618
17	Structure of the CCR5 Chemokine Receptor–HIV Entry Inhibitor Maraviroc Complex. Science, 2013, 341, 1387-1390.	12.6	606
18	Crystal Structure of a Lipid G Protein–Coupled Receptor. Science, 2012, 335, 851-855.	12.6	600

#	Article	IF	CITATIONS
19	Structural Features for Functional Selectivity at Serotonin Receptors. Science, 2013, 340, 615-619.	12.6	600
20	Structural Insights into the Evolution of an Antibody Combining Site. Science, 1997, 276, 1665-1669.	12.6	572
21	Lipidic cubic phase injector facilitates membrane protein serial femtosecond crystallography. Nature Communications, 2014, 5, 3309.	12.8	505
22	Structure of a Class C GPCR Metabotropic Glutamate Receptor 1 Bound to an Allosteric Modulator. Science, 2014, 344, 58-64.	12.6	476
23	Structural Adaptations in a Membrane Enzyme That Terminates Endocannabinoid Signaling. Science, 2002, 298, 1793-1796.	12.6	473
24	Crystal Structure of the Human Cannabinoid Receptor CB1. Cell, 2016, 167, 750-762.e14.	28.9	468
25	Structural Basis for Molecular Recognition at Serotonin Receptors. Science, 2013, 340, 610-614.	12.6	454
26	Molecular control of δ-opioid receptor signalling. Nature, 2014, 506, 191-196.	27.8	432
27	Structure of the nociceptin/orphanin FQ receptor in complex with a peptide mimetic. Nature, 2012, 485, 395-399.	27.8	430
28	Serial Femtosecond Crystallography of G Protein–Coupled Receptors. Science, 2013, 342, 1521-1524.	12.6	424
29	How Ligands Illuminate GPCR Molecular Pharmacology. Cell, 2017, 170, 414-427.	28.9	419
30	Allosteric sodium in class A GPCR signaling. Trends in Biochemical Sciences, 2014, 39, 233-244.	7.5	417
31	Structure of the human smoothened receptor bound to an antitumour agent. Nature, 2013, 497, 338-343.	27.8	415
32	Diversity and modularity of G protein-coupled receptor structures. Trends in Pharmacological Sciences, 2012, 33, 17-27.	8.7	403
33	Microscale Fluorescent Thermal Stability Assay for Membrane Proteins. Structure, 2008, 16, 351-359.	3.3	402
34	Discovery and Characterization of a Highly Selective FAAH Inhibitor that Reduces Inflammatory Pain. Chemistry and Biology, 2009, 16, 411-420.	6.0	401
35	Structural genomics of the Thermotoga maritima proteome implemented in a high-throughput structure determination pipeline. Proceedings of the National Academy of Sciences of the United States of America, 2002, 99, 11664-11669.	7.1	397
36	Ultrasensitive magnetic biosensor for homogeneous immunoassay. Proceedings of the National Academy of Sciences of the United States of America, 2000, 97, 14268-14272.	7.1	387

#	Article	IF	CITATIONS
37	Generic GPCR residue numbers – aligning topology maps while minding the gaps. Trends in Pharmacological Sciences, 2015, 36, 22-31.	8.7	387
38	Crystal structures of agonist-bound human cannabinoid receptor CB1. Nature, 2017, 547, 468-471.	27.8	379
39	Fusion Partner Toolchest for the Stabilization and Crystallization of G Protein-Coupled Receptors. Structure, 2012, 20, 967-976.	3.3	367
40	Severe acute respiratory syndrome coronavirus papain-like protease: Structure of a viral deubiquitinating enzyme. Proceedings of the National Academy of Sciences of the United States of America, 2006, 103, 5717-5722.	7.1	356
41	Structure of the human glucagon class B G-protein-coupled receptor. Nature, 2013, 499, 444-449.	27.8	352
42	Identification of Phosphorylation Codes for Arrestin Recruitment by G Protein-Coupled Receptors. Cell, 2017, 170, 457-469.e13.	28.9	344
43	Conserved Binding Mode of Human β ₂ Adrenergic Receptor Inverse Agonists and Antagonist Revealed by X-ray Crystallography. Journal of the American Chemical Society, 2010, 132, 11443-11445.	13.7	342
44	Common activation mechanism of class A GPCRs. ELife, 2019, 8, .	6.0	339
45	Structure of the human P2Y12 receptor in complex with an antithrombotic drug. Nature, 2014, 509, 115-118.	27.8	330
46	Crystal structure of the chemokine receptor CXCR4 in complex with a viral chemokine. Science, 2015, 347, 1117-1122.	12.6	325
47	Cholera Toxin Binding Affinity and Specificity for Gangliosides Determined by Surface Plasmon Resonanceâ€. Biochemistry, 1996, 35, 6375-6384.	2.5	321
48	Structure of the Angiotensin Receptor Revealed by Serial Femtosecond Crystallography. Cell, 2015, 161, 833-844.	28.9	315
49	Two disparate ligand-binding sites in the human P2Y1 receptor. Nature, 2015, 520, 317-321.	27.8	305
50	Sequence homology and structural analysis of the clostridial neurotoxins. Journal of Molecular Biology, 1999, 291, 1091-1104.	4.2	303
51	Structureâ^'Activity Relationship Studies of Novel Carbocyclic Influenza Neuraminidase Inhibitors. Journal of Medicinal Chemistry, 1998, 41, 2451-2460.	6.4	301
52	Structure of the Nanobody-Stabilized Active State of the Kappa Opioid Receptor. Cell, 2018, 172, 55-67.e15.	28.9	299
53	Agonist-bound structure of the human P2Y12 receptor. Nature, 2014, 509, 119-122.	27.8	279
54	Status of GPCR Modeling and Docking as Reflected by Community-wide GPCR Dock 2010 Assessment. Structure, 2011, 19, 1108-1126.	3.3	269

#	Article	IF	CITATIONS
55	Crystal Structure of the Human Cannabinoid Receptor CB2. Cell, 2019, 176, 459-467.e13.	28.9	268
56	Community-wide assessment of GPCR structure modelling and ligand docking: GPCR Dock 2008. Nature Reviews Drug Discovery, 2009, 8, 455-463.	46.4	260
57	The GPCR Network: a large-scale collaboration to determine human GPCR structure and function. Nature Reviews Drug Discovery, 2013, 12, 25-34.	46.4	252
58	Crystal structure of tyrosine hydroxylase at 2.3 Ã and its implications for inherited neurodegenerative diseases. Nature Structural Biology, 1997, 4, 578-585.	9.7	244
59	A â€~litmus test' for molecular recognition using artificial membranes. Chemistry and Biology, 1996, 3, 113-120.	6.0	236
60	Structure-Based Discovery of Novel Chemotypes for Adenosine A _{2A} Receptor Antagonists. Journal of Medicinal Chemistry, 2010, 53, 1799-1809.	6.4	231
61	An approach to rapid protein crystallization using nanodroplets. Journal of Applied Crystallography, 2002, 35, 278-281.	4.5	227
62	Predicting the emergence of antibiotic resistance by directed evolution and structural analysis. Nature Structural Biology, 2001, 8, 238-242.	9.7	223
63	High-throughput protein crystallization. Current Opinion in Structural Biology, 2000, 10, 558-563.	5.7	221
64	Structure of CC chemokine receptor 2 with orthosteric and allosteric antagonists. Nature, 2016, 540, 458-461.	27.8	220
65	Insights into the structure of class B GPCRs. Trends in Pharmacological Sciences, 2014, 35, 12-22.	8.7	218
66	Crystal structure of the anti-viral APOBEC3G catalytic domain and functional implications. Nature, 2008, 456, 121-124.	27.8	213
67	Design of high-throughput methods of protein production for structural biology. Structure, 2000, 8, R177-R185.	3.3	208
68	Structural basis for Smoothened receptor modulation and chemoresistance to anticancer drugs. Nature Communications, 2014, 5, 4355.	12.8	208
69	Structural basis of autoregulation of phenylalanine hydroxylase. Nature Structural Biology, 1999, 6, 442-448.	9.7	199
70	Global Efforts in Structural Genomics. Science, 2001, 294, 89-92.	12.6	195
71	Human GLP-1 receptor transmembrane domain structure in complex with allosteric modulators. Nature, 2017, 546, 312-315.	27.8	192
72	Structural basis of cell surface receptor recognition by botulinum neurotoxin B. Nature, 2006, 444, 1096-1100.	27.8	190

#	Article	IF	CITATIONS
73	Crystal Structure-Based Virtual Screening for Fragment-like Ligands of the Human Histamine H ₁ Receptor. Journal of Medicinal Chemistry, 2011, 54, 8195-8206.	6.4	189
74	5-HT2C Receptor Structures Reveal the Structural Basis of GPCR Polypharmacology. Cell, 2018, 172, 719-730.e14.	28.9	185
75	Sphingosine-1-Phosphate and Its Receptors: Structure, Signaling, and Influence. Annual Review of Biochemistry, 2013, 82, 637-662.	11.1	184
76	Discovery of New GPCR Biology: One Receptor Structure at a Time. Structure, 2009, 17, 8-14.	3.3	180
77	Structure of the full-length glucagon class B G-protein-coupled receptor. Nature, 2017, 546, 259-264.	27.8	179
78	Opportunities and Challenges in Building a Spatiotemporal Multi-scale Model of the Human Pancreatic β Cell. Cell, 2018, 173, 11-19.	28.9	179
79	Charge-Induced Chromatic Transition of Amino Acid-Derivatized Polydiacetylene Liposomes. Langmuir, 1998, 14, 1974-1976.	3.5	177
80	Structural Basis of Severe Acute Respiratory Syndrome Coronavirus ADP-Ribose-1″-Phosphate Dephosphorylation by a Conserved Domain of nsP3. Structure, 2005, 13, 1665-1675.	3.3	175
81	Structural basis for selectivity and diversity in angiotensin II receptors. Nature, 2017, 544, 327-332.	27.8	174
82	Allosteric Coupling of Drug Binding and Intracellular Signaling in the A2A Adenosine Receptor. Cell, 2018, 172, 68-80.e12.	28.9	173
83	Immunological Origins of Binding and Catalysis in a Diels-Alderase Antibody. Science, 1998, 279, 1929-1933.	12.6	172
84	Crystal Structure of Antagonist Bound Human Lysophosphatidic Acid Receptor 1. Cell, 2015, 161, 1633-1643.	28.9	169
85	Structural Insight into the Aromatic Amino Acid Hydroxylases and Their Disease-Related Mutant Forms. Chemical Reviews, 1999, 99, 2137-2160.	47.7	167
86	Proteomics Analysis Unravels the Functional Repertoire of Coronavirus Nonstructural Protein 3. Journal of Virology, 2008, 82, 5279-5294.	3.4	167
87	Molecular evolution of antibody cross-reactivity for two subtypes of type A botulinum neurotoxin. Nature Biotechnology, 2007, 25, 107-116.	17.5	165
88	Modulating Artificial Membrane Morphology:Â pH-Induced Chromatic Transition and Nanostructural Transformation of a Bolaamphiphilic Conjugated Polymer from Blue Helical Ribbons to Red Nanofibers. Journal of the American Chemical Society, 2001, 123, 3205-3213.	13.7	164
89	Three-Dimensional Structure of Human Tryptophan Hydroxylase and Its Implications for the Biosynthesis of the Neurotransmitters Serotonin and Melatonin [,] . Biochemistry, 2002, 41, 12569-12574.	2.5	164
90	Crystal structure of the catalytic domain of human phenylalanine hydroxylase reveals the structural basis for phenylketonuria. Nature Structural Biology, 1997, 4, 995-1000.	9.7	162

#	Article	IF	CITATIONS
91	Genetically Encoded Chemical Probes in Cells Reveal the Binding Path of Urocortin-I to CRF Class B GPCR. Cell, 2013, 155, 1258-1269.	28.9	159
92	Automation of X-ray crystallography. Nature Structural Biology, 2000, 7, 973-977.	9.7	158
93	Molecular genetics of tetrahydrobiopterin-responsive phenylalanine hydroxylase deficiency. Human Mutation, 2008, 29, 167-175.	2.5	158
94	From The Cover: Correction of kinetic and stability defects by tetrahydrobiopterin in phenylketonuria patients with certain phenylalanine hydroxylase mutations. Proceedings of the National Academy of Sciences of the United States of America, 2004, 101, 16903-16908.	7.1	156
95	Structural basis for bifunctional peptide recognition at human Î ² -opioid receptor. Nature Structural and Molecular Biology, 2015, 22, 265-268.	8.2	151
96	Crystal Structure of Botulinum Neurotoxin Type A in Complex with the Cell Surface Co-Receptor GT1b—Insight into the Toxin–Neuron Interaction. PLoS Pathogens, 2008, 4, e1000129.	4.7	150
97	Advances in GPCR Modeling Evaluated by the GPCR Dock 2013 Assessment: Meeting New Challenges. Structure, 2014, 22, 1120-1139.	3.3	149
98	Structure of CC Chemokine Receptor 5 with a Potent Chemokine Antagonist Reveals Mechanisms of Chemokine Recognition and Molecular Mimicry by HIV. Immunity, 2017, 46, 1005-1017.e5.	14.3	148
99	Structural Basis for Ligand Recognition and Functional Selectivity at Angiotensin Receptor. Journal of Biological Chemistry, 2015, 290, 29127-29139.	3.4	145
100	Rastering strategy for screening and centring of microcrystal samples of human membrane proteins with a sub-10 µm size X-ray synchrotron beam. Journal of the Royal Society Interface, 2009, 6, S587-97.	3.4	144
101	Rapid refinement of crystallographic protein construct definition employing enhanced hydrogen/deuterium exchange MS. Proceedings of the National Academy of Sciences of the United States of America, 2004, 101, 751-756.	7.1	141
102	Structural consequences of effector binding to the T state of aspartate carbamoyltransferase: crystal structures of the unligated and ATP- and CTP-complexed enzymes at 2.6ANG. resolution. Biochemistry, 1990, 29, 7691-7701.	2.5	140
103	Crystal Structure of Tyrosine Hydroxylase with Bound Cofactor Analogue and Iron at 2.3 Ã Resolution:  Self-Hydroxylation of Phe300 and the Pterin-Binding Site,. Biochemistry, 1998, 37, 13437-13445.	2.5	140
104	Structural basis of ligand recognition at the human MT1 melatonin receptor. Nature, 2019, 569, 284-288.	27.8	140
105	Structure of Tetrameric Human Phenylalanine Hydroxylase and Its Implications for Phenylketonuria. Journal of Biological Chemistry, 1998, 273, 16962-16967.	3.4	137
106	Structural Connection between Activation Microswitch and Allosteric Sodium Site in GPCR Signaling. Structure, 2018, 26, 259-269.e5.	3.3	134
107	The Structural Basis of Phenylketonuria. Molecular Genetics and Metabolism, 1999, 68, 103-125.	1.1	132
108	Structure-guided inhibitor design for human FAAH by interspecies active site conversion. Proceedings of the National Academy of Sciences of the United States of America, 2008, 105, 12820-12824.	7.1	132

#	Article	IF	CITATIONS
109	Ligand-Dependent Perturbation of the Conformational Ensemble for the GPCR β2 Adrenergic Receptor Revealed by HDX. Structure, 2011, 19, 1424-1432.	3.3	129
110	Coupling of an induced fit enzyme to polydiacetylene thin films: Colorimetric detection of glucose. Advanced Materials, 1997, 9, 481-483.	21.0	128
111	Steroid-based facial amphiphiles for stabilization and crystallization of membrane proteins. Proceedings of the National Academy of Sciences of the United States of America, 2013, 110, E1203-11.	7.1	127
112	Ribonucleocapsid Formation of Severe Acute Respiratory Syndrome Coronavirus through Molecular Action of the N-Terminal Domain of N Protein. Journal of Virology, 2007, 81, 3913-3921.	3.4	125
113	Stabilization of the Human β2-Adrenergic Receptor TM4–TM3–TM5 Helix Interface by Mutagenesis of Glu1223.41, A Critical Residue in GPCR Structure. Journal of Molecular Biology, 2008, 376, 1305-1319.	4.2	125
114	PAHdb 2003: What a locus-specific knowledgebase can do. Human Mutation, 2003, 21, 333-344.	2.5	124
115	A Structural Perspective of the Sequence Variability Within Botulinum Neurotoxin Subtypes A1-A4. Journal of Molecular Biology, 2006, 362, 733-742.	4.2	122
116	Biophysical Characterization of the Stability of the 150-Kilodalton Botulinum Toxin, the Nontoxic Component, and the 900-Kilodalton Botulinum Toxin Complex Species. Infection and Immunity, 1998, 66, 2420-2425.	2.2	121
117	Cocrystal structure of synaptobrevin-II bound to botulinum neurotoxin type B at 2.0 A resolution. , 2000, 7, 687-692.		119
118	An electrostatic mechanism for Ca2+-mediated regulation of gap junction channels. Nature Communications, 2016, 7, 8770.	12.8	119
119	The genesis of high-throughput structure-based drug discovery using protein crystallography. Current Opinion in Chemical Biology, 2002, 6, 704-710.	6.1	118
120	The Role of a Sodium Ion Binding Site in the Allosteric Modulation of the A2A Adenosine G Protein-Coupled Receptor. Structure, 2013, 21, 2175-2185.	3.3	118
121	Concept of the H(δ+)â<¯ H(δ–) interaction. A low-temperature neutron diffraction study of cis-[IrH(OH)(PMe3)4]PF6. Journal of the Chemical Society Dalton Transactions, 1990, , 1429-1432.	1.1	117
122	Structural Plasticity and the Evolution of Antibody Affinity and Specificity. Journal of Molecular Biology, 2003, 330, 651-656.	4.2	116
123	Dynamics of the β ₂ -Adrenergic G-Protein Coupled Receptor Revealed by Hydrogenâ^'Deuterium Exchange. Analytical Chemistry, 2010, 82, 1100-1108.	6.5	115
124	Time-Controlled Microfluidic Seeding in nL-Volume Droplets To Separate Nucleation and Growth Stages of Protein Crystallization. Angewandte Chemie - International Edition, 2006, 45, 8156-8160.	13.8	113
125	Constitutive phospholipid scramblase activity of a G protein-coupled receptor. Nature Communications, 2014, 5, 5115.	12.8	112
126	Blue-Fluorescent Antibodies. Science, 2000, 290, 307-313.	12.6	110

#	Article	IF	CITATIONS
127	Crystal Structure of Nonstructural Protein 10 from the Severe Acute Respiratory Syndrome Coronavirus Reveals a Novel Fold with Two Zinc-Binding Motifs. Journal of Virology, 2006, 80, 7894-7901.	3.4	110
128	Engineered nanostructured β-sheet peptides protect membrane proteins. Nature Methods, 2013, 10, 759-761.	19.0	110
129	Conformational states of the full-length glucagon receptor. Nature Communications, 2015, 6, 7859.	12.8	110
130	Mechanisms underlying responsiveness to tetrahydrobiopterin in mild phenylketonuria mutations. Human Mutation, 2004, 24, 388-399.	2.5	109
131	Extending the Structural View of Class B GPCRs. Trends in Biochemical Sciences, 2017, 42, 946-960.	7.5	109
132	Structure of the glucagon receptor in complex with a glucagon analogue. Nature, 2018, 553, 106-110.	27.8	109
133	An online resource for GPCR structure determination and analysis. Nature Methods, 2019, 16, 151-162.	19.0	108
134	Crystal Structure and Site-Specific Mutagenesis of Pterin-Bound Human Phenylalanine Hydroxylase [,] . Biochemistry, 2000, 39, 2208-2217.	2.5	106
135	XFEL structures of the human MT2 melatonin receptor reveal the basis of subtype selectivity. Nature, 2019, 569, 289-292.	27.8	106
136	Preclinical evaluation of multiple species of PEGylated recombinant phenylalanine ammonia lyase for the treatment of phenylketonuria. Proceedings of the National Academy of Sciences of the United States of America, 2008, 105, 20894-20899.	7.1	105
137	Crystal structures of aspartate carbamoyltransferase ligated with phosphonoacetamide, malonate, and CTP or ATP at 2.8ANG. resolution and neutral pH. Biochemistry, 1990, 29, 7702-7715.	2.5	104
138	Automated Sample Mounting and Alignment System for Biological Crystallography at a Synchrotron Source. Structure, 2004, 12, 537-545.	3.3	104
139	Protein Biophysical Properties that Correlate with Crystallization Success in Thermotoga maritima: Maximum Clustering Strategy for Structural Genomics. Journal of Molecular Biology, 2004, 344, 977-991.	4.2	102
140	The interplay between binding energy and catalysis in the evolution of a catalytic antibody. Nature, 1997, 389, 271-275.	27.8	101
141	Structural basis of ligand binding modes at the neuropeptide YY1 receptor. Nature, 2018, 556, 520-524.	27.8	100
142	Designing Facial Amphiphiles for the Stabilization of Integral Membrane Proteins. Angewandte Chemie - International Edition, 2007, 46, 7023-7025.	13.8	99
143	Native phasing of x-ray free-electron laser data for a G protein–coupled receptor. Science Advances, 2016, 2, e1600292.	10.3	97
144	Structural Basis for Apelin Control of the Human Apelin Receptor. Structure, 2017, 25, 858-866.e4.	3.3	96

#	Article	IF	CITATIONS
145	A _{2A} adenosine receptor functional states characterized by ¹⁹ F-NMR. Proceedings of the National Academy of Sciences of the United States of America, 2018, 115, 12733-12738.	7.1	96
146	Crystal Structure of Fatty Acid Amide Hydrolase Bound to the Carbamate Inhibitor URB597: Discovery of a Deacylating Water Molecule and Insight into Enzyme Inactivation. Journal of Molecular Biology, 2010, 400, 743-754.	4.2	92
147	Determination of the melanocortin-4 receptor structure identifies Ca ²⁺ as a cofactor for ligand binding. Science, 2020, 368, 428-433.	12.6	89
148	Amino Acid Terminated Polydiacetylene Lipid Microstructures:Â Morphology and Chromatic Transition. Langmuir, 2000, 16, 5333-5342.	3.5	88
149	Single-molecule view of basal activity and activation mechanisms of the G protein-coupled receptor β ₂ AR. Proceedings of the National Academy of Sciences of the United States of America, 2015, 112, 14254-14259.	7.1	87
150	Nucleotides Acting at P2Y Receptors: Connecting Structure and Function. Molecular Pharmacology, 2015, 88, 220-230.	2.3	86
151	Shotgun crystallization strategy for structural genomics: an optimized two-tiered crystallization screen against theThermotoga maritimaproteome. Acta Crystallographica Section D: Biological Crystallography, 2003, 59, 1028-1037.	2.5	85
152	A fully integrated protein crystallization platform for small-molecule drug discovery. Journal of Structural Biology, 2003, 142, 207-217.	2.8	84
153	Binding and Inactivation Mechanism of a Humanized Fatty Acid Amide Hydrolase by α-Ketoheterocycle Inhibitors Revealed from Cocrystal Structures. Journal of the American Chemical Society, 2009, 131, 10497-10506.	13.7	83
154	Ligand Binding and Subtype Selectivity of the Human A2A Adenosine Receptor. Journal of Biological Chemistry, 2010, 285, 13032-13044.	3.4	83
155	Full-length human GLP-1 receptor structure without orthosteric ligands. Nature Communications, 2020, 11, 1272.	12.8	83
156	Expression and Purification of the Saccharomyces cerevisiae α-Factor Receptor (Ste2p), a 7-Transmembrane-segment G Protein-coupled Receptor. Journal of Biological Chemistry, 1997, 272, 15553-15561.	3.4	81
157	In situdata collection and structure refinement from microcapillary protein crystallization. Journal of Applied Crystallography, 2005, 38, 900-905.	4.5	81
158	NMR screening and crystal quality of bacterially expressed prokaryotic and eukaryotic proteins in a structural genomics pipeline. Proceedings of the National Academy of Sciences of the United States of America, 2005, 102, 1901-1905.	7.1	81
159	Fluorine-19 NMR of integral membrane proteins illustrated with studies of GPCRs. Current Opinion in Structural Biology, 2013, 23, 740-747.	5.7	81
160	Crystal structure of a multi-domain human smoothened receptor in complex with a super stabilizing ligand. Nature Communications, 2017, 8, 15383.	12.8	81
161	Elucidating the active δ-opioid receptor crystal structure with peptide and small-molecule agonists. Science Advances, 2019, 5, eaax9115.	10.3	81
162	Organometallic chemistry. 22. Triphenylsilyl perchlorate revisited: silicon-29 and chlorine-35 NMR spectroscopy and x-ray crystallography showing covalent nature in both solution and the solid state. Difficulties in observing long-lived silyl cations in the condensed state. Journal of the American Chemical Society, 1987, 109, 5123-5126.	13.7	80

#	Article	IF	CITATIONS
163	Crystal Structure of a Monomeric Form of Severe Acute Respiratory Syndrome Coronavirus Endonuclease nsp15 Suggests a Role for Hexamerization as an Allosteric Switch. Journal of Virology, 2007, 81, 6700-6708.	3.4	80
164	GPCR stabilization using the bicelle-like architecture of mixed sterol-detergent micelles. Methods, 2011, 55, 310-317.	3.8	80
165	NMR structure and dynamics of the agonist dynorphin peptide bound to the human kappa opioid receptor. Proceedings of the National Academy of Sciences of the United States of America, 2015, 112, 11852-11857.	7.1	80
166	Agonists for 13 Trace Amine-Associated Receptors Provide Insight into the Molecular Basis of Odor Selectivity. ACS Chemical Biology, 2012, 7, 1184-1189.	3.4	79
167	Sodium Ion Binding Pocket Mutations and Adenosine A _{2A} Receptor Function. Molecular Pharmacology, 2015, 87, 305-313.	2.3	79
168	A Single-Domain Llama Antibody Potently Inhibits the Enzymatic Activity of Botulinum Neurotoxin by Binding to the Non-Catalytic α-Exosite Binding Region. Journal of Molecular Biology, 2010, 397, 1106-1118.	4.2	78
169	Structure-Based Ligand Discovery Targeting Orthosteric and Allosteric Pockets of Dopamine Receptors. Molecular Pharmacology, 2013, 84, 794-807.	2.3	78
170	Crystal structure of the Frizzled 4 receptor in a ligand-free state. Nature, 2018, 560, 666-670.	27.8	77
171	Crystal Structure and DNA Binding of the Homeodomain of the Stem Cell Transcription Factor Nanog. Journal of Molecular Biology, 2008, 376, 758-770.	4.2	76
172	Nuclear Magnetic Resonance Structure of the N-Terminal Domain of Nonstructural Protein 3 from the Severe Acute Respiratory Syndrome Coronavirus. Journal of Virology, 2007, 81, 12049-12060.	3.4	75
173	A Comparative Analysis of the Immunological Evolution of Antibody 28B4. Biochemistry, 2001, 40, 10764-10773.	2.5	73
174	Title is missing!. Biomedical Microdevices, 2002, 4, 213-221.	2.8	73
175	β ₂ â€Adrenergic Receptor Activation by Agonists Studied with ¹⁹ Fâ€NMR Spectroscopy. Angewandte Chemie - International Edition, 2013, 52, 10762-10765.	13.8	71
176	Structural and Biochemical Characterization of the Therapeutic Anabaena variabilis Phenylalanine Ammonia Lyase. Journal of Molecular Biology, 2008, 380, 623-635.	4.2	70
177	Identification of Fibroblast Growth Factor Receptor 3 (FGFR3) as a Protein Receptor for Botulinum Neurotoxin Serotype A (BoNT/A). PLoS Pathogens, 2013, 9, e1003369.	4.7	70
178	Crystal structure of the global regulatory protein CsrA from Pseudomonas putida at 2.05 Ã resolution reveals a new fold. Proteins: Structure, Function and Bioinformatics, 2005, 61, 449-453.	2.6	69
179	Exploring the potential impact of an expanded genetic code on protein function. Proceedings of the National Academy of Sciences of the United States of America, 2015, 112, 6961-6966.	7.1	69
180	Structural Comparison of Bacterial and Human Iron-dependent Phenylalanine Hydroxylases: Similar Fold, Different Stability and Reaction Rates. Journal of Molecular Biology, 2002, 320, 645-661.	4.2	68

#	Article	IF	CITATIONS
181	Neutron diffraction structure analysis of a hexanuclear copper hydrido complex, H6Cu6[P(p-tolyl)3]6: an unexpected finding. Journal of the American Chemical Society, 1989, 111, 3472-3473.	13.7	67
182	Chemical Diversity in the G Protein-Coupled Receptor Superfamily. Trends in Pharmacological Sciences, 2018, 39, 494-512.	8.7	67
183	LCP-FRAP Assay for Pre-Screening Membrane Proteins for In Meso Crystallization. Crystal Growth and Design, 2008, 8, 4307-4315.	3.0	65
184	The importance of ligands for G protein-coupled receptor stability. Trends in Biochemical Sciences, 2015, 40, 79-87.	7.5	65
185	Coordinating the impact of structural genomics on the human α-helical transmembrane proteome. Nature Structural and Molecular Biology, 2013, 20, 135-138.	8.2	64
186	The Importance of Ligand-Receptor Conformational Pairs in Stabilization: Spotlight on the N/OFQ G Protein-Coupled Receptor. Structure, 2015, 23, 2291-2299.	3.3	64
187	Crystal structures of the free and liganded form of an esterolytic catalytic antibody 1 1Edited by I. A. Wilson. Journal of Molecular Biology, 1997, 268, 390-400.	4.2	63
188	Unraveling the structures and modes of action of bacterial toxins. Current Opinion in Structural Biology, 1998, 8, 778-784.	5.7	63
189	Crystallographic Analysis of the Human Phenylalanine Hydroxylase Catalytic Domain with Bound Catechol Inhibitors at 2.0 à Resolutionâ€,‡. Biochemistry, 1998, 37, 15638-15646.	2.5	63
190	Partial characterization and three-dimensional-structural localization of eight mutations in exon 7 of the human phenylalanine hydroxylase gene associated with phenylketonuria. FEBS Journal, 1998, 257, 1-10.	0.2	62
191	A Mass Spectrometry Plate Reader: Monitoring Enzyme Activity and Inhibition with a Desorption/Ionization on Silicon (DIOS) Platform. ChemBioChem, 2004, 5, 921-927.	2.6	62
192	Structure of Botulinum Neurotoxin Type D Light Chain at 1.65 à Resolution:  Repercussions for VAMP-2 Substrate Specificity,. Biochemistry, 2006, 45, 3255-3262.	2.5	61
193	Escherichia coli aspartate carbamoyltransferase: the probing of crystal structure analysis via site-specific mutagenesis. Protein Engineering, Design and Selection, 1991, 4, 391-408.	2.1	60
194	Recent Progress in the Structure Determination of GPCRs, a Membrane Protein Family with High Potential as Pharmaceutical Targets. Methods in Molecular Biology, 2010, 654, 141-168.	0.9	60
195	Computational design of thermostabilizing point mutations for G protein-coupled receptors. ELife, 2018, 7, .	6.0	60
196	Crystal Structure of Botulinum Neurotoxin Type G Light Chain:  Serotype Divergence in Substrate Recognition,. Biochemistry, 2005, 44, 9574-9580.	2.5	59
197	The Structure of the Neurotoxin-associated Protein HA33/A from Clostridium botulinum Suggests a Reoccurring β-Trefoil Fold in the Progenitor Toxin Complex. Journal of Molecular Biology, 2005, 346, 1083-1093.	4.2	59
198	LCP-Tm: An Assay to Measure and Understand Stability of Membrane Proteins in a Membrane Environment. Biophysical Journal, 2010, 98, 1539-1548.	0.5	59

#	Article	IF	CITATIONS
199	Structural Genomics of the Severe Acute Respiratory Syndrome Coronavirus: Nuclear Magnetic Resonance Structure of the Protein nsP7. Journal of Virology, 2005, 79, 12905-12913.	3.4	58
200	Structural basis for signal recognition and transduction by platelet-activating-factor receptor. Nature Structural and Molecular Biology, 2018, 25, 488-495.	8.2	58
201	Automatic classification of protein crystallization images using a curve-tracking algorithm. Journal of Applied Crystallography, 2004, 37, 279-287.	4.5	57
202	Structure-based chemical modification strategy for enzyme replacement treatment of phenylketonuria. Molecular Genetics and Metabolism, 2005, 86, 134-140.	1.1	57
203	Converting an injectable protein therapeutic into an oral form: Phenylalanine ammonia lyase for phenylketonuria. Molecular Genetics and Metabolism, 2010, 99, 4-9.	1.1	57
204	Optimization of Adenosine 5′-Carboxamide Derivatives as Adenosine Receptor Agonists Using Structure-Based Ligand Design and Fragment Screening. Journal of Medicinal Chemistry, 2012, 55, 4297-4308.	6.4	57
205	Biopterin responsive phenylalanine hydroxylase deficiency. Genetics in Medicine, 2004, 6, 27-32.	2.4	56
206	Trends in Enzyme Therapy for Phenylketonuria. Molecular Therapy, 2004, 10, 220-224.	8.2	56
207	The Crystal Structure of the α-Neurexin-1 Extracellular Region Reveals a Hinge Point for Mediating Synaptic Adhesion and Function. Structure, 2011, 19, 767-778.	3.3	56
208	Crystallization data mining in structural genomics: using positive and negative results to optimize protein crystallization screens. Methods, 2004, 34, 373-389.	3.8	55
209	Chemotype-selective Modes of Action of κ-Opioid Receptor Agonists. Journal of Biological Chemistry, 2013, 288, 34470-34483.	3.4	55
210	Structural insights into the extracellular recognition of the human serotonin 2B receptor by an antibody. Proceedings of the National Academy of Sciences of the United States of America, 2017, 114, 8223-8228.	7.1	54
211	Structure and Function of Peptide-Binding G Protein-Coupled Receptors. Journal of Molecular Biology, 2017, 429, 2726-2745.	4.2	54
212	Structural and Kinetic Evidence for Strain in Biological Catalysisâ€,‡. Biochemistry, 1998, 37, 14404-14409.	2.5	53
213	X-ray Crystallographic Analysis of α-Ketoheterocycle Inhibitors Bound to a Humanized Variant of Fatty Acid Amide Hydrolase. Journal of Medicinal Chemistry, 2010, 53, 230-240.	6.4	53
214	In vitro expression and analysis of the 826 human G protein-coupled receptors. Protein and Cell, 2016, 7, 325-337.	11.0	53
215	Conformational Effects in Biological Catalysis:  An Antibody-Catalyzed Oxy-Cope Rearrangement. Biochemistry, 2000, 39, 627-632.	2.5	51
216	X-ray laser diffraction for structure determination of the rhodopsin-arrestin complex. Scientific Data, 2016, 3, 160021.	5.3	51

#	Article	IF	CITATIONS
217	NMR Solution Structure of α-Conotoxin ImI and Comparison to Other Conotoxins Specific for Neuronal Nicotinic Acetylcholine Receptorsâ€,‡. Biochemistry, 1999, 38, 3874-3882.	2.5	50
218	Combining structural genomics and enzymology: completing the picture in metabolic pathways and enzyme active sites. Current Opinion in Structural Biology, 2000, 10, 719-730.	5.7	50
219	Crystal structure of thy1, a thymidylate synthase complementing protein fromThermotoga maritimaat 2.25 Ã resolution. Proteins: Structure, Function and Bioinformatics, 2002, 49, 142-145.	2.6	50
220	Structural evidence for substrate strain in antibody catalysis. Proceedings of the National Academy of Sciences of the United States of America, 2003, 100, 856-861.	7.1	50
221	Structure-activity relationships of carbocyclic influenza neuraminidase inhibitors. Bioorganic and Medicinal Chemistry Letters, 1997, 7, 1837-1842.	2.2	49
222	In situX-ray analysis of protein crystals in low-birefringent and X-ray transmissive plastic microchannels. Acta Crystallographica Section D: Biological Crystallography, 2008, 64, 189-197.	2.5	49
223	Microscale NMR Screening of New Detergents for Membrane Protein Structural Biology. Journal of the American Chemical Society, 2008, 130, 7357-7363.	13.7	49
224	Development of an Automated High Throughput LCP-FRAP Assay to Guide Membrane Protein Crystallization in Lipid Mesophases. Crystal Growth and Design, 2011, 11, 1193-1201.	3.0	49
225	The Molecular Mechanism of P2Y ₁ Receptor Activation. Angewandte Chemie - International Edition, 2016, 55, 10331-10335.	13.8	49
226	Amperometric Detection ofEscherichiacoliHeat-Labile Enterotoxin by Redox Diacetylenic Vesicles on a Solâ^'Gel Thin-Film Electrode. Analytical Chemistry, 2000, 72, 1611-1617.	6.5	48
227	Reversible Competitive α-Ketoheterocycle Inhibitors of Fatty Acid Amide Hydrolase Containing Additional Conformational Constraints in the Acyl Side Chain: Orally Active, Long-Acting Analgesics. Journal of Medicinal Chemistry, 2011, 54, 2805-2822.	6.4	48
228	Structural Determinants of Binding the Seven-transmembrane Domain of the Glucagon-like Peptide-1 Receptor (GLP-1R). Journal of Biological Chemistry, 2016, 291, 12991-13004.	3.4	48
229	Emerging structural biology of lipid G proteinâ€coupled receptors. Protein Science, 2019, 28, 292-304.	7.6	46
230	Functional Proteomic and Structural Insights into Molecular Recognition in the Nitrilase Family Enzymes. Biochemistry, 2008, 47, 13514-13523.	2.5	45
231	Structural commonalities among integral membrane enzymes. FEBS Letters, 2004, 567, 159-165.	2.8	44
232	Development of Pegylated Forms of Recombinant Rhodosporidium toruloides Phenylalanine Ammonia-Lyase for the Treatment of Classical Phenylketonuria. Molecular Therapy, 2005, 11, 986-989.	8.2	44
233	Multiple-bond character in Cp3U:CHPMe3: first low-temperature neutron diffraction analysis of a uranium organometallic complex. Organometallics, 1990, 9, 694-697.	2.3	43
234	β 2 -Adrenergic Receptor Conformational Response to Fusion Protein in the Third Intracellular Loop. Structure, 2016, 24, 2190-2197.	3.3	43

#	Article	IF	CITATIONS
235	Human substance P receptor binding mode of the antagonist drug aprepitant by NMR and crystallography. Nature Communications, 2019, 10, 638.	12.8	43
236	Toward PKU Enzyme Replacement Therapy: PEGylation with Activity Retention for Three Forms of Recombinant Phenylalanine Hydroxylase. Molecular Therapy, 2004, 9, 124-129.	8.2	42
237	Modeling ligand recognition at the P2Y12 receptor in light of X-ray structural information. Journal of Computer-Aided Molecular Design, 2015, 29, 737-756.	2.9	42
238	Structure-Based Discovery of New Antagonist and Biased Agonist Chemotypes for the Kappa Opioid Receptor. Journal of Medicinal Chemistry, 2017, 60, 3070-3081.	6.4	42
239	Evaluation of orally administered PEGylated phenylalanine ammonia lyase in mice for the treatment of Phenylketonuria. Molecular Genetics and Metabolism, 2011, 104, 249-254.	1.1	41
240	Extrinsic Tryptophans as NMR Probes of Allosteric Coupling in Membrane Proteins: Application to the A _{2A} Adenosine Receptor. Journal of the American Chemical Society, 2018, 140, 8228-8235.	13.7	41
241	Opportunities for functional selectivity in GPCR antibodies. Biochemical Pharmacology, 2013, 85, 147-152.	4.4	40
242	De Novo Structural Pattern Mining in Cellular Electron Cryotomograms. Structure, 2019, 27, 679-691.e14.	3.3	40
243	Structural Studies on Phenylalanine Hydroxylase and Implications Toward Understanding and Treating Phenylketonuria. Pediatrics, 2003, 112, 1557-1565.	2.1	40
244	Industrializing Structural Biology. Science, 2001, 293, 519-520.	12.6	39
245	Kinetic and stability analysis of PKU mutations identified in BH4-responsive patients. Molecular Genetics and Metabolism, 2005, 86, 11-16.	1.1	38
246	Exploring a 2-Naphthoic Acid Template for the Structure-Based Design of P2Y ₁₄ Receptor Antagonist Molecular Probes. ACS Chemical Biology, 2014, 9, 2833-2842.	3.4	38
247	Profiling of membrane protein variants in a baculovirus system by coupling cell-surface detection with small-scale parallel expression. Protein Expression and Purification, 2007, 56, 85-92.	1.3	37
248	Design, Synthesis, and Properties of Branch-Chained Maltoside Detergents for Stabilization and Crystallization of Integral Membrane Proteins: Human Connexin 26. Langmuir, 2010, 26, 8690-8696.	3.5	36
249	Crystal Structure of the Botulinum Neurotoxin Type G Binding Domain: Insight into Cell Surface Binding. Journal of Molecular Biology, 2010, 397, 1287-1297.	4.2	36
250	Evaluation of Molecular Modeling of Agonist Binding in Light of the Crystallographic Structure of an Agonist-Bound A2A Adenosine Receptor. Journal of Medicinal Chemistry, 2012, 55, 538-552.	6.4	36
251	Trapping a transition state in a computationally designed protein bottle. Science, 2015, 347, 863-867.	12.6	36
252	Visualizing subcellular rearrangements in intact β cells using soft x-ray tomography. Science Advances, 2020, 6, .	10.3	36

#	Article	IF	CITATIONS
253	Biased Signaling of the G-Protein-Coupled Receptor β2AR Is Governed by Conformational Exchange Kinetics. Structure, 2020, 28, 371-377.e3.	3.3	36
254	Aluminum dichloride and dibromide. Preparation, spectroscopic (including matrix isolation) study, reactions, and role (together with alkyl(aryl)aluminum monohalides) in the preparation of organoaluminum compounds. Journal of the American Chemical Society, 1988, 110, 3231-3238.	13.7	35
255	Crystal structure of a tandem cystathionine-β-synthase (CBS) domain protein (TM0935) from Thermotoga maritima at 1.87 A resolution. Proteins: Structure, Function and Bioinformatics, 2004, 57, 213-217.	2.6	35
256	The Structure of a Eukaryotic Nicotinic Acid Phosphoribosyltransferase Reveals Structural Heterogeneity among Type II PRTases. Structure, 2005, 13, 1385-1396.	3.3	35
257	High-throughput x-ray crystallography for structure-based drug design. Drug Discovery Today, 2001, 6, 113-118.	6.4	34
258	Structure-based epitope and PEGylation sites mapping of phenylalanine ammonia-lyase for enzyme substitution treatment of phenylketonuria. Molecular Genetics and Metabolism, 2007, 91, 325-334.	1.1	34
259	Purification, Modeling, and Analysis of Botulinum Neurotoxin Subtype A5 (BoNT/A5) from Clostridium botulinum Strain A661222. Applied and Environmental Microbiology, 2011, 77, 4217-4222.	3.1	34
260	Dynamic Strategic Bond Analysis Yields a Ten-Step Synthesis of 20-nor-Salvinorin A, a Potent κ-OR Agonist. ACS Central Science, 2017, 3, 1329-1336.	11.3	34
261	FoldGPCR: Structure prediction protocol for the transmembrane domain of G proteinâ€coupled receptors from class A. Proteins: Structure, Function and Bioinformatics, 2010, 78, 2189-2201.	2.6	33
262	Fluoride-Mediated Capture of a Noncovalent Bound State of a Reversible Covalent Enzyme Inhibitor: X-ray Crystallographic Analysis of an Exceptionally Potent α-Ketoheterocycle Inhibitor of Fatty Acid Amide Hydrolase. Journal of the American Chemical Society, 2011, 133, 4092-4100.	13.7	33
263	High-throughput identification of G protein-coupled receptor modulators through affinity mass spectrometry screening. Chemical Science, 2018, 9, 3192-3199.	7.4	33
264	Crystal structure of an iron-containing 1,3-propanediol dehydrogenase (TM0920) from Thermotoga maritima at 1.3 Ã resolution. Proteins: Structure, Function and Bioinformatics, 2003, 54, 174-177.	2.6	32
265	Response of patients with phenylketonuria in the US to tetrahydrobiopterin. Molecular Genetics and Metabolism, 2005, 86, 17-21.	1.1	32
266	Towards miniaturization of a structural genomics pipeline using micro-expression and microcoil NMR. Journal of Structural and Functional Genomics, 2006, 6, 259-267.	1.2	32
267	Crystal structure of misoprostol bound to the labor inducer prostaglandin E2 receptor. Nature Chemical Biology, 2019, 15, 11-17.	8.0	32
268	Structural studies on phenylalanine hydroxylase and implications toward understanding and treating phenylketonuria. Pediatrics, 2003, 112, 1557-65.	2.1	32
269	Crystallization and preliminary X-ray analysis of botulinum neurotoxin type A. Journal of Molecular Biology, 1991, 222, 877-880.	4.2	31
270	Rational Design of Fatty Acid Amide Hydrolase Inhibitors That Act by Covalently Bonding to Two Active Site Residues. Journal of the American Chemical Society, 2013, 135, 6289-6299.	13.7	30

#	Article	IF	CITATIONS
271	Structural Basis of the Diversity of Adrenergic Receptors. Cell Reports, 2019, 29, 2929-2935.e4.	6.4	30
272	Structural insights into hormone recognition by the human glucose-dependent insulinotropic polypeptide receptor. ELife, 2021, 10, .	6.0	30
273	Crystal structure of a glycerophosphodiester phosphodiesterase (GDPD) from Thermotoga maritima (TM1621) at 1.60 Ã resolution. Proteins: Structure, Function and Bioinformatics, 2004, 56, 167-170.	2.6	29
274	The N-Terminal Sequence of Tyrosine Hydroxylase Is a Conformationally Versatile Motif That Binds 14-3-3 Proteins and Membranes. Journal of Molecular Biology, 2014, 426, 150-168.	4.2	29
275	Preparation of Stilbene-Tethered Nonnatural Nucleosides for Use with Blue-Fluorescent Antibodies. Journal of Organic Chemistry, 2001, 66, 1725-1732.	3.2	28
276	Scalable high-throughput micro-expression device for recombinant proteins. BioTechniques, 2004, 37, 364-370.	1.8	28
277	Crystal structure of a PIN (PilT N-terminus) domain (AF0591) from Archaeoglobus fulgidus at 1.90 Ã resolution. Proteins: Structure, Function and Bioinformatics, 2004, 56, 404-408.	2.6	28
278	Crystal structure of acireductone dioxygenase (ARD) from Mus musculus at 2.06 Ã resolution. Proteins: Structure, Function and Bioinformatics, 2006, 64, 808-813.	2.6	28
279	Structural aspects of therapeutic enzymes to treat metabolic disorders. Human Mutation, 2009, 30, 1591-1610.	2.5	28
280	Structural Characterization of Three Novel Hydroxamate-Based Zinc Chelating Inhibitors of the <i>Clostridium botulinum</i> Serotype A Neurotoxin Light Chain Metalloprotease Reveals a Compact Binding Site Resulting from 60/70 Loop Flexibility. Biochemistry, 2011, 50, 4019-4028.	2.5	28
281	Structural Basis for BABIM Inhibition of Botulinum Neurotoxin Type B Protease. Journal of the American Chemical Society, 2000, 122, 11268-11269.	13.7	27
282	Crystal structure of a novel manganese-containing cupin (TM1459) from Thermotoga maritima at 1.65 Ã resolution. Proteins: Structure, Function and Bioinformatics, 2004, 56, 611-614.	2.6	27
283	Visualizing insulin vesicle neighborhoods in β cells by cryo–electron tomography. Science Advances, 2020, 6, .	10.3	27
284	Structure-Activity Relationships in a Peptidic α7 Nicotinic Acetylcholine Receptor Antagonist. Journal of Molecular Biology, 2000, 304, 911-926.	4.2	26
285	Robotics for Automated Crystal Formation and Analysis. Methods in Enzymology, 2003, 368, 45-76.	1.0	26
286	Long live structural biology. Nature Structural and Molecular Biology, 2004, 11, 293-295.	8.2	26
287	Advancing Chemokine GPCR Structure Based Drug Discovery. Structure, 2019, 27, 405-408.	3.3	26
288	Monolayer properties of monosialioganglioside in the mixed diacetylene lipid films on the air/water interface. Chemistry and Physics of Lipids, 1997, 87, 41-53.	3.2	25

#	Article	IF	CITATIONS
289	Accelerating the Throughput of Affinity Mass Spectrometry-Based Ligand Screening toward a G Protein-Coupled Receptor. Analytical Chemistry, 2019, 91, 8162-8169.	6.5	25
290	An X-ray and neutron diffraction structure analysis of a triply-bridged binuclear iridium complex, [[(C5(CH3)5Ir)2(μ-H)3]+ [ClO4]â^• 2C6H6]. Inorganica Chimica Acta, 1989, 161, 223-231.	2.4	24
291	Synthesis of site-specific antibody-drug conjugates by ADP-ribosyl cyclases. Science Advances, 2020, 6, eaba6752.	10.3	24
292	Arginine 54 in the active site of escherichia coli aspartate transcarbamoylase is critical for catalysis: A siteâ€specific mutagenesis, NMR, and Xâ€ray crystallographic study. Protein Science, 1992, 1, 1435-1446.	7.6	23
293	Signaling ofEscherichia ColiEnterotoxin on Supramolecular Redox Bilayer Vesicles. Journal of the American Chemical Society, 1999, 121, 6767-6768.	13.7	23
294	Morphological manipulation of bolaamphiphilic polydiacetylene assemblies by controlled lipid doping. Chemistry and Physics of Lipids, 2002, 114, 203-214.	3.2	23
295	Inâ€Membrane Chemical Modification (IMCM) for Siteâ€Specific Chromophore Labeling of GPCRs. Angewandte Chemie - International Edition, 2015, 54, 15246-15249.	13.8	23
296	Identification of natural products as novel ligands for the human 5-HT2C receptor. Biophysics Reports, 2018, 4, 50-61.	0.8	23
297	Synthesis and Properties of Dodecyl Trehaloside Detergents for Membrane Protein Studies. Langmuir, 2012, 28, 11173-11181.	3.5	22
298	Design, synthesis, pharmacological characterization of a fluorescent agonist of the P2Y 14 receptor. Bioorganic and Medicinal Chemistry Letters, 2015, 25, 4733-4739.	2.2	22
299	The Human D1ADopamine Receptor: Heterologous Expression inSaccharomyces cerevisiaeand Purification of the Functional Receptor. Protein Expression and Purification, 1998, 13, 111-119.	1.3	21
300	Crystal structure of an Udp-n-acetylmuramate-alanine ligase MurC (TM0231) from Thermotoga maritima at 2.3 Ã resolution. Proteins: Structure, Function and Bioinformatics, 2004, 55, 1078-1081.	2.6	21
301	Crystal Structure of a Voltage-gated K+ Channel Pore Module in a Closed State in Lipid Membranes. Journal of Biological Chemistry, 2012, 287, 43063-43070.	3.4	21
302	β ₂ â€Adrenergic Receptor Solutions for Structural Biology Analyzed with Microscale NMR Diffusion Measurements. Angewandte Chemie - International Edition, 2013, 52, 331-335.	13.8	21
303	Crystal structure of a type II quinolic acid phosphoribosyltransferase (TM1645) from Thermotoga maritima at 2.50 A resolution. Proteins: Structure, Function and Bioinformatics, 2004, 55, 768-771.	2.6	20
304	Salvianolic acids from antithrombotic Traditional Chinese Medicine Danshen are antagonists of human P2Y1 and P2Y12 receptors. Scientific Reports, 2018, 8, 8084.	3.3	20
305	Biophysical and Ion Channel Functional Characterization of the Torpedo californica Nicotinic Acetylcholine Receptor in Varying Detergent–Lipid Environments. Journal of Membrane Biology, 2008, 223, 13-26.	2.1	19
306	Live-cell imaging of glucose-induced metabolic coupling of β and αÂcell metabolism in health and typeÂ2 diabetes. Communications Biology, 2021, 4, 594.	4.4	19

#	Article	IF	CITATIONS
307	Bayesian metamodeling of complex biological systems across varying representations. Proceedings of the United States of America, 2021, 118, .	7.1	19
308	Crystal structure of O-acetylserine sulfhydrylase (TM0665) from Thermotoga maritima at 1.8 Ã resolution. Proteins: Structure, Function and Bioinformatics, 2004, 56, 387-391.	2.6	18
309	Generation of an Orthogonal Protein–Protein Interface with a Noncanonical Amino Acid. Journal of the American Chemical Society, 2017, 139, 5728-5731.	13.7	18
310	Allosteric control of quaternary states in E. coli aspartate transcarbamylase. Biochemical and Biophysical Research Communications, 1990, 171, 1312-1318.	2.1	17
311	Recombinant Expression and Purification of the Botulinum Neurotoxin Type A Translocation Domain. Protein Expression and Purification, 1997, 11, 195-200.	1.3	17
312	Crystal structure of γ-glutamyl phosphate reductase (TM0293) from Thermotoga maritima at 2.0 Ã resolution. Proteins: Structure, Function and Bioinformatics, 2003, 54, 157-161.	2.6	17
313	Crystal structure of an aspartate aminotransferase (TM1255) from Thermotoga maritima at 1.90 Ã resolution. Proteins: Structure, Function and Bioinformatics, 2004, 55, 759-763.	2.6	17
314	Crystal structure of a putative PII-like signaling protein (TM0021) from Thermotoga maritima at 2.5 Ã resolution. Proteins: Structure, Function and Bioinformatics, 2004, 54, 810-813.	2.6	17
315	Molecular Mechanism for Ligand Recognition and Subtype Selectivity of α2C Adrenergic Receptor. Cell Reports, 2019, 29, 2936-2943.e4.	6.4	17
316	Electron Density Projection Map of the Botulinum Neurotoxin 900-kilodalton Complex by Electron Crystallography. Journal of Structural Biology, 1997, 120, 78-84.	2.8	16
317	Crystal structure of a putative oxalate decarboxylase (TM1287) from Thermotoga maritima at 1.95 Ã resolution. Proteins: Structure, Function and Bioinformatics, 2004, 56, 392-395.	2.6	16
318	Crystal structure of S-adenosylmethionine:tRNA ribosyltransferase-isomerase (QueA) from Thermotoga maritima at 2.0 A resolution reveals a new fold. Proteins: Structure, Function and Bioinformatics, 2005, 59, 869-874.	2.6	16
319	Reduction in diffuso-convective disturbances in nanovolume protein crystallization experiments. Journal of Applied Crystallography, 2005, 38, 87-90.	4.5	15
320	Crystal structure of a single-stranded DNA-binding protein (TM0604) from Thermotoga maritima at 2.60 Ã resolution. Proteins: Structure, Function and Bioinformatics, 2006, 63, 256-260.	2.6	15
321	RAMP-ing up Class-B GPCR ECD Structural Coverage. Structure, 2010, 18, 1067-1068.	3.3	15
322	Facile chemoenzymatic synthesis of a novel stable mimic of NAD ⁺ . Chemical Science, 2018, 9, 8337-8342.	7.4	15
323	A Single Reactive Noncanonical Amino Acid Is Able to Dramatically Stabilize Protein Structure. ACS Chemical Biology, 2019, 14, 1150-1153.	3.4	15
324	A Novel Approach to Quantify G-Protein-Coupled Receptor Dimerization Equilibrium Using Bioluminescence Resonance Energy Transfer. Methods in Molecular Biology, 2013, 1013, 93-127.	0.9	15

#	Article	IF	CITATIONS
325	Location of the elusive hydride ligand in HRh [P(C6H5)3]4 via a neutron diffraction analysis. Inorganica Chimica Acta, 1989, 166, 173-175.	2.4	14
326	Crystal structure of a ribose-5-phosphate isomerase RpiB (TM1080) from Thermotoga maritima at 1.90 Ã resolution. Proteins: Structure, Function and Bioinformatics, 2004, 56, 171-175.	2.6	14
327	Shotgun Crystallization Strategy for Structural Genomics II: Crystallization Conditions that Produce High Resolution Structures for T. maritima Proteins. Journal of Structural and Functional Genomics, 2005, 6, 209-217.	1.2	14
328	Structure of strontium hydroxide octahydrate, Sr(OH)2·8H2O, at 20, 100 and 200â€K from neutron diffraction. Acta Crystallographica Section B: Structural Science, 2005, 61, 381-386.	1.8	14
329	Crystal structure of an alanine-glyoxylate aminotransferase from Anabaena sp. at 1.70 Ã resolution reveals a noncovalently linked PLP cofactor. Proteins: Structure, Function and Bioinformatics, 2005, 58, 971-975.	2.6	14
330	Chaperone-Like Therapy with Tetrahydrobiopterin in Clinical Trials for Phenylketonuria: Is Genotype a Predictor of Response?. JIMD Reports, 2011, 5, 59-70.	1.5	14
331	Single Amino Acid Variation Underlies Species-Specific Sensitivity to Amphibian Skin-Derived Opioid-like Peptides. Chemistry and Biology, 2015, 22, 764-775.	6.0	14
332	Structural insight into apelin receptor-G protein stoichiometry. Nature Structural and Molecular Biology, 2022, 29, 688-697.	8.2	14
333	Crystal structure of an indigoidine synthase A (IndA)-like protein (TM1464) from Thermotoga maritima at 1.90 Ã resolution reveals a new fold. Proteins: Structure, Function and Bioinformatics, 2005, 59, 864-868.	2.6	13
334	Crystal structure of Hsp33 chaperone (TM1394) from Thermotoga maritima at 2.20 Ã resolution. Proteins: Structure, Function and Bioinformatics, 2005, 61, 669-673.	2.6	13
335	Crystal structure of an Apo mRNA decapping enzyme (DcpS) from Mouse at 1.83 Ã resolution. Proteins: Structure, Function and Bioinformatics, 2005, 60, 797-802.	2.6	12
336	Structure-Based Design of Melanocortin 4 Receptor Ligands Based on the SHU-9119-hMC4R Cocrystal Structure. Journal of Medicinal Chemistry, 2021, 64, 357-369.	6.4	12
337	Crystal structure of a phosphoribosylaminoimidazole mutase PurE (TM0446) from Thermotoga maritima at 1.77-Ã resolution. Proteins: Structure, Function and Bioinformatics, 2004, 55, 474-478.	2.6	11
338	Crystal structure of an $\hat{l}\pm/\hat{l}^2$ serine hydrolase (YDR428C) from Saccharomyces cerevisiae at 1.85 Å resolution. Proteins: Structure, Function and Bioinformatics, 2004, 58, 755-758.	2.6	11
339	Protein Crystallization in Restricted Geometry: Advancing Old Ideas for Modern Times in Structural Proteomics. Methods in Molecular Biology, 2008, 426, 363-376.	0.9	11
340	Crystal structure of a putative modulator of DNA gyrase (pmbA) from Thermotoga maritima at 1.95 Ã resolution reveals a new fold. Proteins: Structure, Function and Bioinformatics, 2005, 61, 444-448.	2.6	10
341	Crystal structure of the ApbE protein (TM1553) from Thermotoga maritima at 1.58 Ã resolution. Proteins: Structure, Function and Bioinformatics, 2006, 64, 1083-1090.	2.6	10
342	Crystal structure of a glycerate kinase (TM1585) from Thermotoga maritima at 2.70 Ã resolution reveals a new fold. Proteins: Structure, Function and Bioinformatics, 2006, 65, 243-248.	2.6	10

#	Article	IF	CITATIONS
343	Rescue of Misfolded Proteins and Stabilization by Small Molecules. Methods in Molecular Biology, 2010, 648, 313-324.	0.9	10
344	The lipid phase preference of the adenosine A _{2A} receptor depends on its ligand binding state. Chemical Communications, 2019, 55, 5724-5727.	4.1	10
345	An orthogonal seryl-tRNA synthetase/tRNA pair for noncanonical amino acid mutagenesis in Escherichia coli. Bioorganic and Medicinal Chemistry, 2020, 28, 115662.	3.0	10
346	Crystal structure of a putative NADPH-dependent oxidoreductase (GI: 18204011) from mouse at 2.10 Ã resolution. Proteins: Structure, Function and Bioinformatics, 2004, 56, 629-633.	2.6	9
347	Crystallization Optimum Solubility Screening: using crystallization results to identify the optimal buffer for protein crystal formation. Acta Crystallographica Section F: Structural Biology Communications, 2005, 61, 1035-1038.	0.7	9
348	Crystal structure of a conserved hypothetical protein (gi: 13879369) from Mouse at 1.90 Ã resolution reveals a new fold. Proteins: Structure, Function and Bioinformatics, 2005, 61, 1132-1136.	2.6	9
349	Mutations in the Regulatory Domain of Phenylalanine Hydroxylase and Response to Tetrahydrobiopterin. Genetic Testing and Molecular Biomarkers, 2007, 11, 174-178.	1.7	9
350	Crystal structure of 2â€ketoâ€3â€deoxygluconate kinase (TM0067) from <i>Thermotoga maritima</i> at 2.05 à resolution. Proteins: Structure, Function and Bioinformatics, 2008, 70, 603-608.	2.6	9
351	A structurally guided dissection-then-evolution strategy for ligand optimization of smoothened receptor. MedChemComm, 2017, 8, 1332-1336.	3.4	9
352	Rational Remodeling of Atypical Scaffolds for the Design of Photoswitchable Cannabinoid Receptor Tools. Journal of Medicinal Chemistry, 2021, 64, 13752-13765.	6.4	9
353	Importance of a conserved residue, aspartate-162, for the function of Escherichia coli aspartate transcarbamoylase. Biochemistry, 1992, 31, 3026-3032.	2.5	8
354	Crystal structure of a zinc-containing glycerol dehydrogenase (TM0423) from Thermotoga maritima at 1.5 Ã resolution. Proteins: Structure, Function and Bioinformatics, 2002, 50, 371-374.	2.6	8
355	Crystal structure of uronate isomerase (TM0064) fromThermotoga maritimaat 2.85 Ã resolution. Proteins: Structure, Function and Bioinformatics, 2003, 53, 142-145.	2.6	8
356	Crystal structure of a methionine aminopeptidase (TM1478) from Thermotoga maritima at 1.9 Ã resolution. Proteins: Structure, Function and Bioinformatics, 2004, 56, 396-400.	2.6	8
357	Crystal structure of an orphan protein (TM0875) from Thermotoga maritima at 2.00-Ã resolution reveals a new fold. Proteins: Structure, Function and Bioinformatics, 2004, 56, 607-610.	2.6	8
358	Comparative structural analysis of a novel glutathioneS-transferase (ATU5508) fromAgrobacterium tumefaciensat 2.0 Ã resolution. Proteins: Structure, Function and Bioinformatics, 2006, 65, 527-537.	2.6	8
359	Correlation of inhibitor effects on enzyme activity and thermal stability for the integral membrane protein fatty acid amide hydrolase. Bioorganic and Medicinal Chemistry Letters, 2008, 18, 5847-5850.	2.2	8
360	Small-scale approach for precrystallization screening in GPCR X-ray crystallography. Nature Protocols, 2020, 15, 144-160.	12.0	8

#	Article	IF	CITATIONS
361	Pursuing High-Resolution Structures of Nicotinic Acetylcholine Receptors: Lessons Learned from Five Decades. Molecules, 2021, 26, 5753.	3.8	8
362	Response to Rupp and Segelke. Nature Structural Biology, 2001, 8, 664-664.	9.7	7
363	Structural analysis of affinity matured antibodies and laboratory-evolved enzymes. Advances in Protein Chemistry, 2001, 55, 227-259.	4.4	7
364	Crystal structure of an HEPN domain protein (TM0613) from Thermotoga maritima at 1.75 Ã resolution. Proteins: Structure, Function and Bioinformatics, 2004, 54, 806-809.	2.6	7
365	Crystal structure of phosphoribosylformylglycinamidine synthase II (smPurL) from Thermotoga maritima at 2.15 A resolution. Proteins: Structure, Function and Bioinformatics, 2006, 63, 1106-1111.	2.6	7
366	Crystal structure of an ORFan protein (TM1622) fromThermotoga maritimaat 1.75 Ã resolution reveals a fold similar to the Ran-binding protein Mog1p. Proteins: Structure, Function and Bioinformatics, 2006, 65, 777-782.	2.6	7
367	Crystal structure of a novel Thermotoga maritima enzyme (TM1112) from the cupin family at 1.83 Ã resolution. Proteins: Structure, Function and Bioinformatics, 2004, 56, 615-618.	2.6	6
368	Crystal structure of a putative glutamine amido transferase (TM1158) from Thermotoga maritima at 1.7 à resolution. Proteins: Structure, Function and Bioinformatics, 2004, 54, 801-805.	2.6	6
369	Crystal structure of virulence factor CJ0248 from Campylobacter jejuni at 2.25 Ã resolution reveals a new fold. Proteins: Structure, Function and Bioinformatics, 2005, 62, 292-296.	2.6	6
370	Crystal structure of TM1367 from Thermotoga maritima at 1.90 Ã resolution reveals an atypical member of the cyclophilin (peptidylprolyl isomerase) fold. Proteins: Structure, Function and Bioinformatics, 2006, 63, 1112-1118.	2.6	6
371	Crystal structure of phosphoribosylformyl-glycinamidine synthase II, PurS subunit (TM1244) from Thermotoga maritima at 1.90 Ã resolution. Proteins: Structure, Function and Bioinformatics, 2006, 65, 249-254.	2.6	6
372	Generation of Protein Structures for the 21st Century. Structure, 2007, 15, 1517-1519.	3.3	5
373	Growth and excitement in membrane protein structural biology. Current Opinion in Structural Biology, 2010, 20, 399-400.	5.7	5
374	Trapping Small Caffeine in a Large GPCR Pocket. Structure, 2011, 19, 1204-1207.	3.3	5
375	The structure-based traceless specific fluorescence labeling of the smoothened receptor. Organic and Biomolecular Chemistry, 2019, 17, 6136-6142.	2.8	5
376	Auto-segmentation and time-dependent systematic analysis of mesoscale cellular structure in β-cells during insulin secretion. PLoS ONE, 2022, 17, e0265567.	2.5	5
377	Structural Studies of Catalytic Antibodies. Israel Journal of Chemistry, 1996, 36, 121-132.	2.3	4
378	Crystal structure of a formiminotetrahydrofolate cyclodeaminase (TM1560) from Thermotoga maritima at 2.80 Ã resolution reveals a new fold. Proteins: Structure, Function and Bioinformatics, 2005, 58, 976-981.	2.6	4

#	Article	IF	CITATIONS
379	Probing the CB ₁ Cannabinoid Receptor Binding Pocket with AM6538, a High-Affinity Irreversible Antagonist. Molecular Pharmacology, 2019, 96, 619-628.	2.3	4
380	Crystal structure of 2-phosphosulfolactate phosphatase (ComB) fromClostridium acetobutylicumat 2.6 Ã resolution reveals a new fold with a novel active site. Proteins: Structure, Function and Bioinformatics, 2006, 65, 771-776.	2.6	3
381	Neural Network Segmentation of Cell Ultrastructure Using Incomplete Annotation. , 2020, , .		3
382	Synthesis of Linear Acetylenic Carbon. Tanso, 1998, 1998, 27-33.	0.1	3
383	Transition metal methylene complexes. Journal of Organometallic Chemistry, 1991, 412, 425-434.	1.8	2
384	Crystal structure of an allantoicase (YIR029W) from Saccharomyces cerevisiae at 2.4 Ã resolution. Proteins: Structure, Function and Bioinformatics, 2004, 56, 619-624.	2.6	2
385	Five Years of Increasing Structural Biology Throughput - A Retrospective Analysis. , 2007, , 1-26.		2
386	A roadmap to membrane protein structures. Methods, 2011, 55, 271-272.	3.8	2
387	The Molecular Mechanism of P2Y ₁ Receptor Activation. Angewandte Chemie, 2016, 128, 10487-10491.	2.0	2
388	Assessment of scoring functions to rank the quality of 3D subtomogram clusters from cryo-electron tomography. Journal of Structural Biology, 2021, 213, 107727.	2.8	2
389	A new visual design language for biological structures in a cell. Structure, 2022, , .	3.3	2
390	Design of an inverted spindle axis for frozen crystal screening and storage. Journal of Applied Crystallography, 1996, 29, 738-740.	4.5	1
391	Monolayer and epi-fluorescence microscopy studies of amino acid derivatized diacetylene lipids. Thin Solid Films, 1999, 345, 292-299.	1.8	1
392	Regulatory properties of tetrahydrobiopterin cofactor bound at the active site of phenylalanine hydroxylase. Pteridines, 2000, 11, 34-36.	0.5	1
393	Structural Studies of the Human Kappa Opioid Receptor Active State Conformations. Biophysical Journal, 2016, 110, 38a-39a.	0.5	1
394	Low Resolution Model of Botulinum Neurotoxin Type A. , 1993, , 393-395.		1
395	Synthesis of linear acetylenic carbon; The fourth carbon allotrope. Carbon, 1998, 36, 1248.	10.3	0
396	Functional Amphiphilic and Bolaamphiphilic Poly(diacetylene) Assemblies with Controlled Optical and Morphological Properties. ACS Symposium Series, 2004, , 96-109.	0.5	0

#	Article	IF	Citations
397	SPINE forward. Acta Crystallographica Section D: Biological Crystallography, 2006, 62, iii-iii.	2.5	0
398	The Importance of Target Selection Strategies in Structural Biology. , 2008, , 1-27.		0
399	G Protein-Coupled Receptor Structures. , 2010, , 129-138.		0
400	Asia growth in membrane protein structure. Current Opinion in Structural Biology, 2013, 23, 481-482.	5.7	0
401	THE SEVEN TRANSMEMBRANE SUPERFAMILY. , 2014, , .		0
402	Conformational Dynamics of a G Protein-Coupled Receptor at the Single-Molecule Level. Biophysical Journal, 2015, 108, 350a.	0.5	0
403	Biochemical Characterization and Structure Determination of the Class C TAS1R Subfamily of Chemosensory Receptors. Biophysical Journal, 2016, 110, 395a.	0.5	0
404	Mesoscale Architecture of Beta Cells Upon Glucose and Ex-4 Stimulation. Biophysical Journal, 2019, 116, 431a.	0.5	0
405	Towards a Model of the Human Pancreatic Beta Cell. Biophysical Journal, 2019, 116, 451a.	0.5	0
406	Biased Signaling Pathways in β ₂ -Adrenergic Receptor Characterized by ¹⁹ F-NMR. , 2021, , 179-183.		0
407	Allosteric Coupling of Drug Binding and Intracellular Signaling in the A2A Adenosine Receptor. , 2021, , 184-196.		0
408	""Smart―Materials for Colorimetric Detection of Pathogenic Agents. , 2002, , .		0
409	Triphenylsilyl Perchlorate Revisited: ²⁹ Si and ³⁵ Cl NMR Spectroscopy and X-ray Crystallography Showing Covalent Nature in Both Solution and the Solid State. Difficulties in Observing Long-Lived Silyl Cations in the Condensed State. World Scientific Series in 20th Century Chemistry. 2003 1112-1115.	0.0	0
410	Crystal Structures of the β2-Adrenergic Receptor. NATO Science for Peace and Security Series A: Chemistry and Biology, 2009, , 217-230.	0.5	0
411	Structure and Function of the Gâ€protein Coupled Receptor Family. FASEB Journal, 2010, 24, lb230.	0.5	0
412	Allosteric Coupling of Drug Binding and Intracellular Signaling in the A _{2A} Adenosine Receptor. SSRN Electronic Journal, 0, , .	0.4	0
413	Globally Monitoring Allosteric Coupling in the A _{2A} Adenosine Receptor by NMR in Solution. FASEB Journal, 2018, 32, 533.99.	0.5	0
414	Towards Generating Spatiotemporal Multiscale Models of Human Pancreatic Beta Cells. Diabetes, 2018, 67, .	0.6	0